AIAA 80-1205R

# Fluid Mechanics of Deflagration-to-Detonation Transition in Porous Explosives and Propellants

Stephen J. Hoffman* and Herman Krier†
*University of Illinois at Urbana-Champaign, Urbana, Ill.*

**The fluid mechanical processes which characterize a transition from deflagration to detonation in granular beds of solid propellant have not at present been sufficiently refined to allow accurate modeling of the phenomenon. In an attempt to improve this situation, this paper reports on the investigation of the basic mechanisms and consequences that arise from a set of assumptions for the governing and constitutive equations which take into account the two-phase nature of this problem. A qualitative description of the flow process is made, based on observations obtained from deflagration-to-detonation transition (DDT) experiments. From this, certain conclusions are reached as to the properties needed by propellants to exhibit a deflagration-to-detonation transition. The numerical integration scheme itself is examined in detail in order to further understand the consequences of its use. Also, two scenarios for DDT are presented which exhibit characteristics similar to those derived from experimental evidence. Conclusions as to the direction of future research are made based on the results obtained from the work which led to these two basic mechanisms for DDT.**

## I. Description of the Fluid Dynamics of DDT

### Introduction

THE work presented in this paper is a continuation of research to determine a mechanism which explains deflagration-to-detonation transition (DDT) in porous reactive solids. The specific regime under consideration is the DDT phenomenon observed in tightly packed beds of finely granulated, highly energetic solid propellants, a description of which can be found in Krier and Gokhale[1] with further results to be found in Krier et al.[2,3]

The method used in analyzing this problem is basically the same as that developed in Krier and Kezerle,[2] namely, the use of six conservation equations based on the concept of separated continuum flow for both the gas and solid phases.

In addition to these conservation equations, state equations for both the gas and the solid phases of the bed will be used to make the computer simulation as realistic as possible. In this case, the gas state equation has been formulated to provide accurate results in the nonideal, high-pressure flow which is under consideration. The use of a state equation for the solid phase, which represents an improvement over the incompressible assumption used in previous works, will allow variations in the particle density to take place.

Owing to the separated nature of the flow, there must be supplemental constitutive laws that account for the interaction of the two phases of the flow. These laws take into account such factors as an interphase heat transfer and a gas-particle drag. In the studies reported, Krier-Gokhale[1] and Krier-Kezerle,[2] a compaction resistance law was used that later proved to be unsatisfactory when subsequent calculations were made for packed beds of increasing length.[3] This has since been modified to correct this difficulty. Each individual phase also has a set of constitutive relations which are necessary to describe the flow completely. These include such equations as a law describing the axial particle stress (related to the compaction resistance law), a model to describe the movement of this stress wave, a pressure-dependent burning rate law for the particles, and a temperature-dependent gas viscosity law. Variations in any one of these constitutive laws cause their own change in the progression of the flow through the bed. Results from the variations in some of these laws will be presented.

### Deflagration-to-Detonation Transition (DDT)

Experimental studies of the spontaneous DDT in a packed bed of granular or solid propellant indicates that in the steady-state detonation phase, a pressure shock wave precedes the flame (or ignition) front. One mechanism for DDT is made clear in the work by Bernecker and Price,[4] which assumes that the pressure front (not yet a shock wave) is initially behind the flame front. But due to the rapid generation of gases by the burning propellant, the pressure front is simultaneously increased in magnitude, steepened in its gradient, and accelerated toward the flame front. The point at which the pressure front overtakes the flame front is then defined as the transition point, after which the flame front, now preceded by the pressure front, moves down the bed in a self-sustaining detonation wave at a speed greater than the deflagration wave. Normally one would expect that the formation of the incipient shock wave that becomes a detonation would have required a compaction of the bed with the associated drastic reduction in bed porosity (see Ref. 5). Such compaction arises from rearrangement of the particles, plastic flow, and, most likely, fracture of the particles.

The analysis made in this paper does not include complexities such as those just mentioned, although some modeling attempts are summarized in a previous report.[6] However, it is not necessarily true that rapid gas generation with flame spreading at high rates cannot of itself provide local shock development, a condition necessary for a detonation to occur.

### Areas of Investigation

The work presented in Krier and Kezerle[2] developed the necessary conservation equations and constitutive laws to perform the predetonation fluid dynamics, which is a necessary part of either of the previously mentioned DDT models. Using this set of laws, an effort to find the DDT mechanism based on the first mechanism was made by utilizing a selective variation of parameters in this set of equations. The results of this effort seemed to indicate that unless some alternative jump-like function were introduced in

Presented as Paper 80-1205 at the AIAA/SAE/ASME 16th Joint Propulsion Conference, Hartford, Conn., June 30-July 2, 1980; submitted Sept. 12, 1980; revision received May 15, 1981. 

*Graduate Teaching Assistant, Dept. of Aeronautical and Astronautical Engineering. Student Member AIAA.

†Professor, Dept. of Mechanical and Industrial Engineering. Associate Fellow AIAA.

the equations, one does not predict the formation of a reaction front which is moving at speeds in the range of 5-10 mm/$\mu$s and is being supported by the advance in the detonation shock. Some candidates that include the physics to allow for such a jump-like function are the following concepts:

1) At some critical high pressure $P^*$, or at some critical $(dP/dt)^*$, the material burns at a "super" rate different from the rates assumed and extrapolated from the lower pressure data base.

2) Since the burning rate $\dot{r}$ appears only in the mass generation term $\Gamma$, it should logically follow that one should look at other terms in $\Gamma$ for use as a discontinuous type function. For example, since $\Gamma=\rho_p\dot{r}(1-\phi)(3/r_p)$, one might wish to formulate a state equation in which either density $\rho_p$ or solids loading $(1-\phi)$ increases discontinuously, at some high (critical) pressure.

3) Again looking at the $\Gamma$ term, one could assume that, at a given instant, a critical pressure could fracture the particles, thereby drastically increasing the surface to volume ratio $(3r_p)$.

With regard to the model for DDT, the codes developed and used by Krier-Gokhale[1] and Krier-Kezerle[2] made use of a compaction resistance law that was a function of only the porosity $\phi$, which could be interpreted as the particle stress. Due to the nature of the equations, the minimum porosity always occurred in association with the gas pressure front. Thus the stress wave would not propagate into the bed in a manner similar to a compression wave, but would merely remain tied to the gas pressure front. In order to obtain the presumed stress wave motion, it was determined that the particle stress would need to be predicted in such a way as to correct the problem encountered earlier in the longer length beds and to decouple the motion of the stress wave from the motion of the gas pressure front. This was accomplished by locating the point of maximum stress (presumed to be a function of both gas pressure and the drag force) and allowing that stress to propagate forward at a sound speed associated with that stress. Since there are no distinct viscosity type terms associated with the solid-phase equations that would normally account for the motion of this type of disturbance, it was felt that imposing this kind of assumption on the stress wave would simply be a shorthand way of describing the dynamic compression of a "homogeneous solid."

In general, the method of investigation presented here is constructed in such a manner so as to provide conditions in which the DDT phenomenon can manifest itself. This is done by assuming that a fraction of the propellant grains are ignited at one end of a closed chamber. The mass generated in the ignition region accelerates the resulting hot gases forward, with the region behind these hot gases rapidly increasing in pressure. This pressure rise is due to the large quantities of gaseous material generated when the propellant is assumed to obey a pressure-sensitive burning rate law. At this point it is presumed that one of the two transition mechanisms (see Ref. 6) will cause the bed to exhibit a DDT. Regardless of the mechanism that causes the transition, a detonation can be said to have begun when the very strong pressure front precedes the flame front and both move through the bed at a speed which is characteristic of a detonation wave for the type of propellant and initial porosity used. In this paper, the flame front will be defined as the locus of points that mark the position in the bed of the initial particle ignition. The definition of the pressure front will depend on the transition mechanism being considered and thus will be deferred until Sec. III, in which particular cases will be discussed in detail.

## II. Governing Equations for Unsteady, One-Dimensional, Two-Phase Flow

The conservation equations that make up the governing balances for both the gas and particle phase are, for the most part, the same as those found in Krier and Kezerle.[2] But significant changes have been made in key constitutive laws that provide closure for the model. As mentioned earlier, the approach taken in developing the conservation equations assumes that there are two distinct continua, one for solids and one for the gas, each moving through its own control volume. Owing to this approach the sum of these two volumes must represent an average mixture volume, while at the same time the equations which describe the two continua must account for the effect that one flow has on the other. To obtain this, distinct equations for continuity, momentum, and energy are written for each phase which recognize that each phase occupies only part of the total volume and utilizes inertial-coupling terms that disappear when the two sets of equations are summed together. A detailed derivation of these equations, along with the assumptions required, are presented in Krier and Kezerle.[2] However, owing to the two detonation mechanism theories being considered, certain modifications must be included and will be noted when made.

### Conservation Equations

In order to uniquely describe the properties of the two-phase flow, the following nine variables must be determined: $\rho_g$, $\rho_p$, $u_g$, $u_p$, $T_g$, $T_p$, $P_g$, $P_p$, and $\phi$. For these nine unknowns, nine equations must be supplied, and the following conservation equations for the assumed one-dimensional, two-phase flow provide six of the necessary relations:

Gas continuity

$$\frac{\partial\rho_1}{\partial t}=-\frac{\partial(\rho_1 u_g)}{\partial x}+\Gamma \tag{1}$$

Solid continuity

$$\frac{\partial\rho_2}{\partial t}=-\frac{\partial(\rho_2 u_p)}{\partial x}-\Gamma \tag{2}$$

Gas momentum

$$\frac{\partial(\rho_1 u_g)}{\partial t}=-\frac{\partial(\rho_1 u_g^2)}{\partial x}-\phi\frac{\partial P_g}{\partial x}-\bar{F}+\Gamma u_p \tag{3}$$

Solid momentum

$$\frac{\partial(\rho_2 u_p)}{\partial t}=-\frac{\partial(\rho_2 u_p^2)}{\partial x}-(1-\phi)\frac{\partial P_p}{\partial x}+\bar{F}-\Gamma u_p \tag{4}$$

Gas energy

$$\frac{\partial(E_{g_T}\rho_1)}{\partial t}=-\frac{\partial(u_g E_{g_T}\rho_1+u_g\phi P_g)}{\partial x}$$
$$+\Gamma\left(\frac{u_p^2}{2}+E_g^{\text{chem}}\right)-\bar{F}u_p-\dot{Q} \tag{5}$$

Particle energy

$$\frac{\partial(E_{p_T}\rho_2)}{\partial t}=-\frac{\partial(u_p E_{p_T}\rho_2+u_p(1-\phi)P_p)}{\partial x}$$
$$+\Gamma\left(\frac{-u_p^2}{2}+E_p^{\text{chem}}\right)+\bar{F}u_p+\dot{Q} \tag{6}$$

where we define the following:

Phase densities

$$\rho_1=\phi\rho_g,\quad \rho_2=(1-\phi)\rho_p \tag{7a}$$

Porosity

$$\phi = V_g / V_{\text{mix}}$$

solid loading: (7b)

$$1-\phi = V_p / V_{\text{mix}}$$

Total internal energy (gas)

$$E_{g_T} = E_g + \tfrac{1}{2}u_g^2 \quad \text{and} \quad E_g = c_{v_g} T_g \tag{7c}$$

Total internal energy (particles)

$$E_{p_T} = E_p + \tfrac{1}{2}u_p^2 \quad \text{and} \quad E_p = c_{v_p} T_p \tag{7d}$$

where subscripts $g$ and $p$ denote the gas and particle phase, respectively. Here $c_v = 1.269$ and 1.777 kJ/kg K (0.30316 and 0.42442 Btu/lbm°R). Both are assumed average constants, independent of temperature. $E^{\text{chem}}$ refers to the chemical energy released in burning.

The seventh and eighth equations needed are the equations of state associated with each phase. For the gas, a Nobel-Able type of nonideal equation of state is used, i.e.,

$$P_g = \rho_g R_g T_g / (1 - \rho_g B_v) \tag{8}$$

where $B_v$ is the covolume, a term that is a function of gas density. In this study it is assumed that

$$1/(1-\rho_g B_v) = a + b\rho_g + d\rho_g^2 + d\rho_g^3 \tag{9}$$

where $a = 1.0$, $b = 1.0$, $c = 0.5$, $d = 0.3$, and $\rho_g$ is in g/cm$^3$. This equation results from an assumption that the gas particles behave as hard spheres during any interaction. One can show that Eq. (7c) will give the gas internal energy given the form of Eqs. (8) and (9). An equation of state for the solid phase is included and will be discussed later.

#### Constitutive Relations for $P_p$

As described by Wallis,[7] a packed bed placed under a compressive load can be further compacted. However, there is a force which resists this compaction that depends on the stress-strain relationship of the particle lattice, which is not necessarily the same as that of a homogeneous solid made from the same material. The compressive load on the bed will be split between the two phases in proportion to the porosity. So the resultant force on the particles will be a function of the porosity, the porosity gradient, and possibly other factors. There can be a variety of formulations that could be used to relate this particle-particle interaction through a stress, which is termed here as $P_p$ (Refs. 8 and 9). Formulations that give $P_p = P_p(\phi)$, such as the one found in Ref. 8, are open to question, since this type of function allows the bulk modulus of the particle lattice to decrease as the porosity increases.[6] The exact opposite should be the case.

For this paper, it has been assumed that the particles maintain a spherical geometry throughout compaction. We have thus artificially imposed the constraint that the normal stress $P_p$ be a functional relation that resists compaction below a porosity of 0.2595 (Ref. 6). It is understood that this approach has little physical justification but is consistent with other assumptions made thus far. A logical progression at this point is to allow compaction beyond the just mentioned porosity by treating nonspherical particles and using the resistance data available in the literature (Ref. 9).

#### Additional Constitutive Relations

In order to complete the analysis of Eqs. (1-6) it is necessary to define certain criteria and interaction laws with the use of known physical relationships or through the use of experimentally established laws. These include

1) an ignition criterion based on the bulk temperature of the particles;

2) the propellant burning rate, $\dot{r}_p$;

3) the gas generation rate, $\Gamma$, which for spherical particles is

$$\Gamma = (3/r_p)(1-\phi)\rho \dot{r}_p \tag{10}$$

4) the interphase heat transfer rate, $\dot{Q}$, which is defined as

$$\dot{Q} = h_{pg}(T_g - T_p)(\phi)(S/V)_p \tag{11}$$

where $(S/V)_p$ is the surface to volume ratio for the particles and $h_{pg}$ is the interphase heat transfer coefficient, which is discussed in the Appendix;

5) the interphase drag, $\bar{F}$, which is defined as

$$\bar{F} = [\mu(U_g - U_p)(1-\phi)^2 / 4r_p^2 \phi^2] f_{pg} \tag{12}$$

where $\mu$ is the gas phase viscosity and $f_{pg}$ is the interphase drag coefficient which is a required input. Packed bed correlations that constrain $f_{pg}$ are discussed in Refs. 1-3 and 6.

#### Numerical Integration Technique

In order to solve this set of hyperbolic nonlinear partial differential equations, the two-step predictor-corrector numerical integration scheme developed by MacCormack was used. This is the same type of scheme as detailed in Ref. 2, with a few exceptions which will be outlined below.

Throughout this investigation the total bed length was usually set at 7.62 cm (3 in.) with the $\Delta x$ set at 0.0127 cm (0.05 in.). This value of $\Delta x$ was determined to provide the largest allowable mesh size for repeatable calculations. The value of $L = 7.62$ cm (3 in.) gave moderate computing charges. The $\Delta t$ (for this $\Delta x$) is calculated using the Courant, Friedrichs, Levy stability criterion, namely,

$$\Delta t(C + |u|)/\Delta x \leq 1 \tag{13}$$

Here, $C$ and $|u|$ are the maximum gas phase or solid phase sound speed and phase velocity, respectively, and not the mixture average values as utilized by Krier and Kezerle.[2] This was done to provide more stable solutions for all classes of problems studied here. To satisfy the inequality in Eq. (13) the value of unity was set equal to 0.7.

Even with the use of a guaranteed stability criterion for the linear form of the hyperbolic equations, there were conditions under which the computer code would become unstable for our nonlinear set of equations. Although it was found that these instabilities, caused by severe gradients in one or more of the partial differential equations, could be removed in some cases by utilizing a smaller $\Delta x$ (and its associated reduced $\Delta t$), an artificial smoothing routine was adopted to insure stability. A detailed discussion of this smoothing technique can be found in Ref. 10. Thus, most of the results presented here did not employ artificial smoothing and hence the range of input parameters was often limited.

The boundary conditions chosen for this investigation are the same as those used by Krier and Kezerle with the exception of the choice of gradients at the wall. In this present work the code was programmed to insure that all gradient terms at both end walls are zero at all times.

The *initial* conditions as utilized in this investigation were imposed to begin a flow process in a closed configuration. The choice for some of the initial conditions was somewhat arbitrary. The modeling attempts to specify a minimum energy impulse to initiate the convective flow, which will not necessarily predetermine the following flow events. Specifically,

1) The particle temperature was set to exceed the ignition temperature $T_p$ in the first small fraction of the bed. At the same time the gas temperature $T_g$ was set to the flame temperature of the combustibles.

**Table 1 Typical input data**

| Parameter | Value SIU | Value English |
|---|---|---|
| Initial bed temperature, $T_g, T_p$ | 294 K | 530°R |
| Ignition energy, $\Delta E_{\text{ign}}$ | 383 kJ/kg | 165 Btu/lbm |
| Ignition temperature, $T_{\text{ign}}$ | 303 K | 545°R |
| Initial bed porosity | 0.4 | 0.4 |
| Propellant burning rate constant, $b_1$ | $3.32\times10^{-7}$ cm/s-Pa$^n$ | $9.0\times10^{-4}$ in./s-psi$^n$ |
| Propellant burning rate index, $n$ | 0.90 | 0.90 |
| Initial propellant density, $\rho_p$ | 1.581 g/cm$^3$ | 0.0571 lbm/in.$^3$ |
| Initial bulk modulus, $K_0$ | 1.38 GPa | $2.00\times10^5$ lbf/in. |
| Constant volume specific heat of the propellant, $c_{v_p}$ | 1.2665 J/g·K | 0.30316 Btu/lbm°R |
| Initial grain radius, $r_p$ | 0.1016 mm | $4.0\times10^{-3}$ in. |
| Chemical energy released, $E_{\text{chem}}=(E_g-E_p)^{\text{chem}}$ | 5479.6 kJ/kg | 2360.9 Btu/lbm |
| Molecular weight of the gas, MW | | 22.6 lbm/lbmole |
| Covolume of propellant gas, $B_v$ | 1.078 cm$^3$/g | 29.85 in.$^3$/lbm |
| Specific heat ratio of gas, $\gamma$ | 1.252 | 1.252 |
| Constant volume specific heat of gas, $c_{v_g}$ | 1.7731 Joule/g-K | 0.42442 Btu/lbm°R |
| Gas viscosity, $\mu_g$ | $4.45\times10^{-4}$ g/cm-s | $2.49\times10^{-6}$ lbm/in.-s |
| Universal gas constant, $\bar{R}$ | 8.3005 Joule/g-K | 1.9869 Btu/lbmole°R |
| Total bed length, $L_B$ | 76.2 mm | 3.0 in. |
| Percent heat transfer to particle after ignition | 10% | 10% |

2) The gas pressure, $P_g$ was assumed to drop exponentially to an ambient value from an assumed moderately high pressure at $x=0$. In many cases the pressure was alternately set at a *uniform* low ambient pressure.

3) Velocities of both phases were set to zero over the entire length of the bed.

4) The porosity was set at some selected value (typically $\phi_0=0.4$) which was also uniform across the total bed length.

## III. Computed Results

### Introduction

As discussed in Sec. I, the investigations described in this report consist of a more detailed analysis of the fluid mechanical properties leading up to the detonation transition of a porous reactive bed as opposed to those studies carried out by Krier-Gokhale[1] and Krier-Kezerle.[2] Specifically, changes in the solid phase conservation equations used by Krier and Kezerle were made in an attempt to gain a better understanding of the properties of a bed of closely packed particles and to determine what conditions are required for this bed to exhibit a DDT. These changes included the addition of a solid-phase state equation, the definition and use of a particle pressure, and modifications to some of the various constitutive laws which are necessary to completely describe the flow. A discussion of the effects of each of these changes on the unsteady fluid dynamics in the bed will be presented below.

However, to provide a comparison with the calculations presented in the earlier works of Krier-Gokhale and Krier-Kezerle, a baseline case was constructed to closely reflect typical results found in these studies. Table 1 lists the most important inputs for both the baseline calculation and for the subsequent parameter variation calculations. The results of these calculations will be presented using one or more of the following graphical formats: pressure, temperature, and porosity vs distance, and the ignition front position (flame front) vs time.

### Baseline Case

An initial baseline case was constructed where it is assumed that the solid phase is incompressible and that the packed bed obeys the particle-particle interaction law developed by Kuo-Summerfield.[8] An initial uniform porosity of 0.40 (solids loading of 60%) was used. The report by Hoffman and Krier[6] presents additional details concerned with the effect of boundary conditions and assumed grid step sizes $\Delta x$ (and resulting $\Delta t$) which optimizes the computation, as far as accuracy and computation time are concerned.

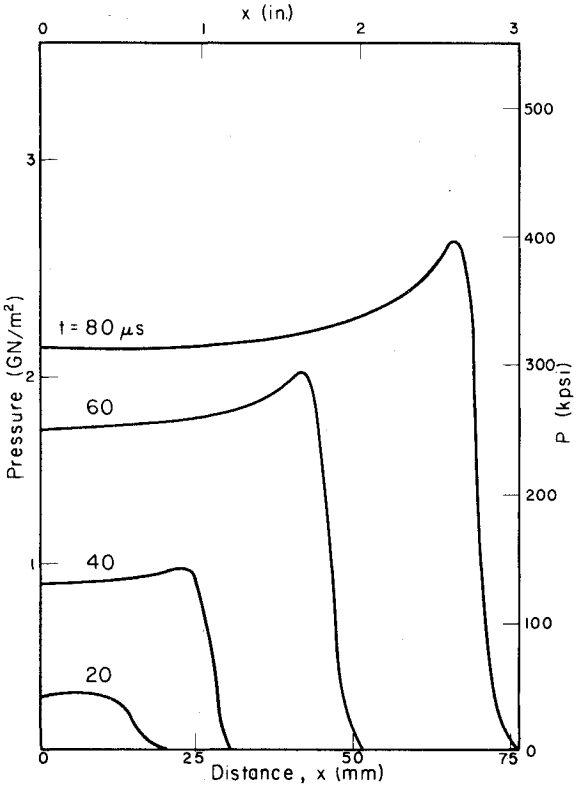


**Fig. 1 Pressure distribution during flame spreading in an initially packed bed of small particles of solid propellant. (Figures 2-4 show variation in other flow parameters for the same case as calculated for Fig. 1.)**

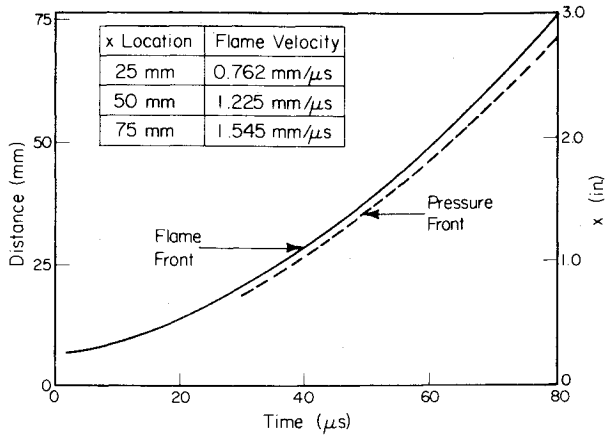


**Fig. 2 Locus of ignition (flame) front and pressure front, the latter derived from pressure vs distance distribution (incompressible solid).**

The development of the gas pressure distribution (Fig. 1) obviously is similar to that presented by Krier and Kezerle in that the pressure front shows a distinct tendency to build into a continental divide. A continental divide is defined here as a gas pressure spike which usually appears in the region of the deflagration front. This spike is significant in that the pressure gradients which have now been formed will cause the gas to move both toward and away from the burning zone. The reason that such a divide forms is due to the continuing availability of gas volume in the section initially ignited as the propellant burns away in an ever accelerating manner as the pressure rises. A typical value for this gradient at $t=60$ μs and $x=44.5$ mm (1.75 in.) is of the order of $-0.3136$ GPa/mm ($-1.16\times10^6$ psi/in.).

Figure 2 shows the progression of the ignition point through the bed; this locus is defined as the flame front. The pressure front as shown in this figure was defined as being the locus of points midway between the peak of the continental divide and the ambient pressure level in front of the buildup.

A comparison of the particle and gas temperature development is shown in Fig. 3. Again, the continental divide structure seen in the gas temperature presented in Krier-Kezerle is seen here. The severe gas temperature spike seen at 80 μs is due more to the encounter of pressure reflection with the end wall than to some drastic change in the progression of the deflagration wave. It should be noted that no disassociation of the gases is assumed in these calculations. If real gas properties were being assumed, temperatures of this magnitude (i.e., 4000 K or greater) would certainly cause the gases to dissociate, reducing the high values predicted. The particle temperature profiles exhibit a structure similar to those presented in Ref. 2, i.e., no continental divide, but the magnitude of the temperature at later times during the convective flow sequence was brought about by the extremely small volume taken up by the solid phase (porosities of 0.96 or greater) and the high temperature of the surrounding gas. Under such conditions, even the restricted heat transfer from the gas (10% after ignition) causes a tremendous increase in the temperature of the particles. Since it was felt that this type of phenomenon was a product of the calculation procedure and not in fact real, subsequent cases remove all heat transfer at the higher levels of porosity ($\phi\geq0.96$). Even with the extremely high particle temperature exhibited in this case, the progress of the convective process has not been affected since the particle phase at this point is an insignificant fraction of the flow.

The porosity distribution (Fig. 4) exhibits a contour which is characterized by a zone in which the material is compressed to a porosity lower than the original value. The point of lowest porosity is always located ahead of the peak pressure point, but it should be noted that the compressed zone does not prevent the point of first ignition from moving through

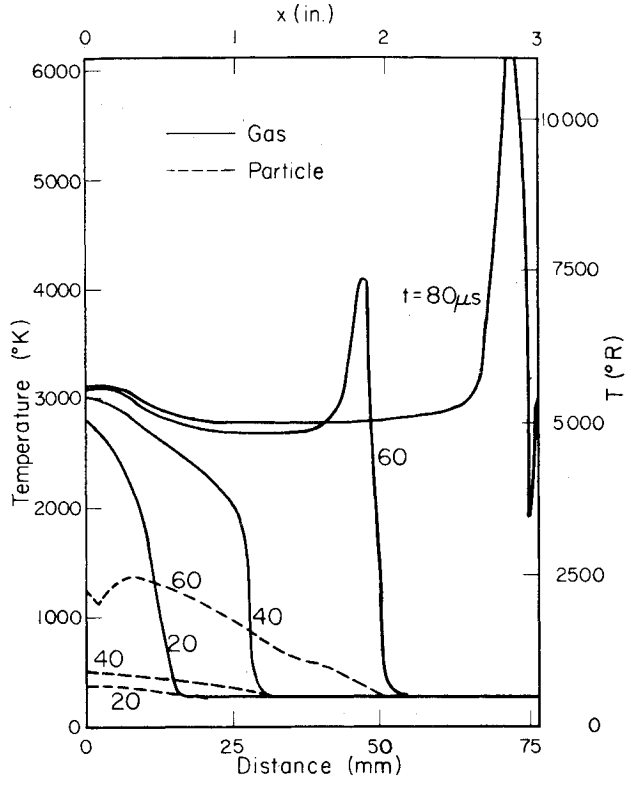


**Fig. 3 Gas and particle temperature distribution history.**

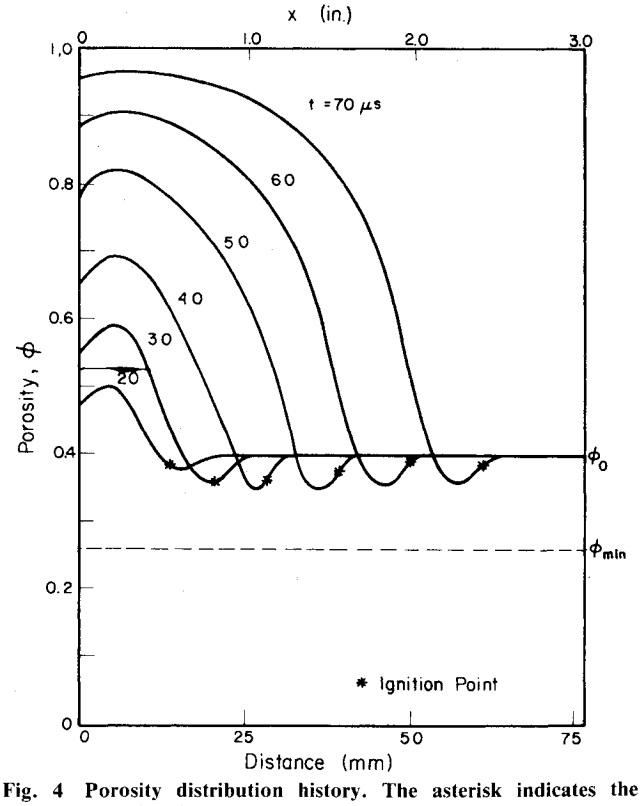


**Fig. 4 Porosity distribution history. The asterisk indicates the location of the ignition front.**

this zone. This ignition point was always found to occur at relatively low gas temperature, typically less than 600 K. It would seem that the bed would need to be much more severely compacted to prevent any hot gases from "seeping through" before a significant pressure can be built up behind the ignition front. This seems to be a prerequisite for transition to detonation.

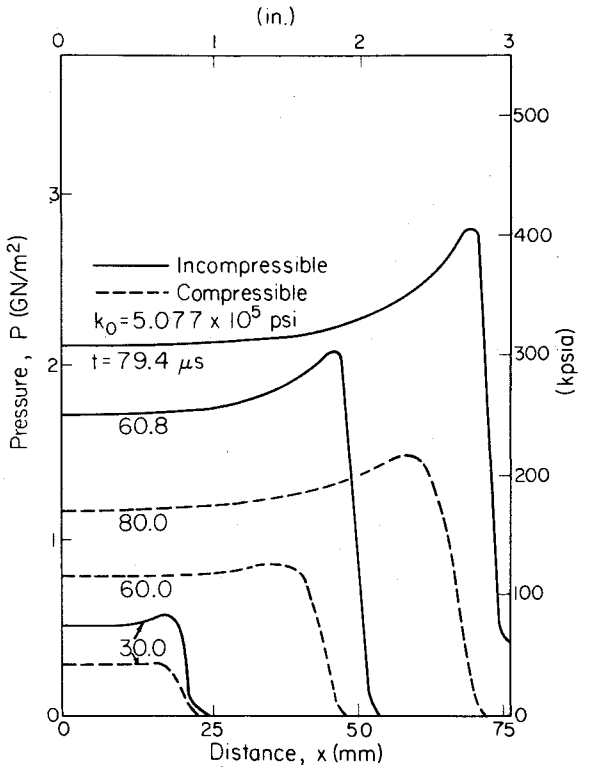


**Fig. 5 Pressure distribution history comparing the incompressible solid to a compressible material.**

### Variation in Propellant Properties

The assumption of an incompressible solid is one reason for such relatively high pressures. A possible remedy for this situation is a reduction in the volume taken up by the solids, thus leaving a larger volume into which the gas can expand. This can be accomplished by assuming that the particles are compressible. As mentioned earlier, a modified Tait equation gives

$$\rho_p = \rho_{0_p}\left[\frac{3P}{K_0} + 1\right]^{1/3} \tag{14}$$

At 0.69 GPa (100,000 psi), $\rho/\rho_0 = 1.36$ for $K_0 = 1.38$ GPa (200,000 psi), a soft plastic. In order to conserve the particle mass as the density increases, the particle size must decrease according to the ratio $r/r_0 = (\rho/\rho_0)^{1/3}$. At 0.69 GPa, the reduction is $r/r_0 = 2/5$.

Figure 5 shows the drastic reduction in the gas pressure that is predicted with the inclusion of this particle state equation. At any particular time, the magnitude of that pressure is nearly cut in half. Surprisingly, there is no significant reduction in the time needed to completely ignite the bed. The flame front slope decreases slightly (on the order of 10%) for the compressible solid case. This is caused by the fact that the decrease in particle radius allows an increase in bed porosity which allows more hot gases to move farther into the bed in a shorter period of time. However, the lower gas pressures and pressure gradients caused by this increase in porosity have exactly the opposite effect in that the acceleration terms in the gas momentum equation are reduced, yielding lower forward gas velocities. The net effect of these two phenomena is effectively to cancel each other out, thus causing little change in the flame front curve.

The significant lowering of the gas pressure also has its effect on the temperatures within the bed. The gas temperatures are reduced to much more reasonable levels when compared to results obtained from a comparable incompressible case. The sensitivity of $K_0$ on the resulting gas pressure levels and ignition fronts are discussed in Ref. 6.

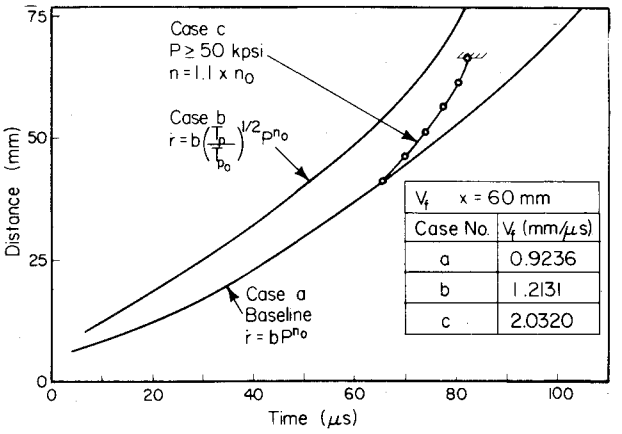


**Fig. 6 Flame front locus as a function of burning rate.**

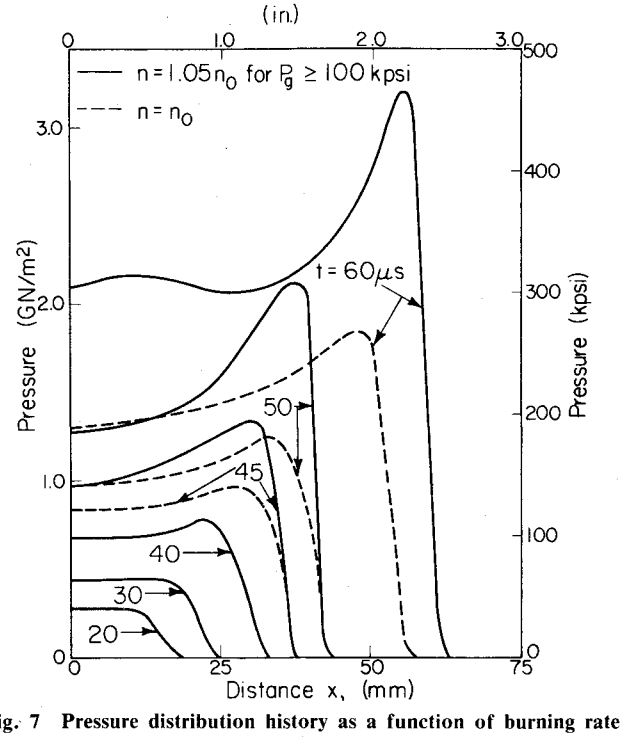


**Fig. 7 Pressure distribution history as a function of burning rate exponent change.**

### Mechanisms for the Gas Generation Function

As discussed in Sec. I, in order to develop a strong pressure shock and an expected abrupt change in the flame velocity, one could model a rapid increase in one of the components of the mass generation term, Γ, at some assumed critically high pressure or in some region of excess solids compaction. The term Γ (mass/volume-time) for spherical particles burning on their outer surfaces only was expressed as Eq. (10), where

$$\dot{r} = \text{propellant burning rate} = (T_p/T_{p_0})(bP^n) \tag{15}$$

Equation (10) allows for a number of possible changes to be modeled in the individual components or combinations of components at some preselected critical condition.

Figure 6 shows the results from two of these possibilities. Case a represents the unperturbed prediction of the flame front locus. Case b illustrates the enhancement of the flame moving through the bed by simply increasing Γ throughout the run. In this case the enhancement was the result of allowing the propellant burning rate to be augmented by the magnitude of the propellant temperature increase. The second case (case c) made use of an increase in the pressure exponent

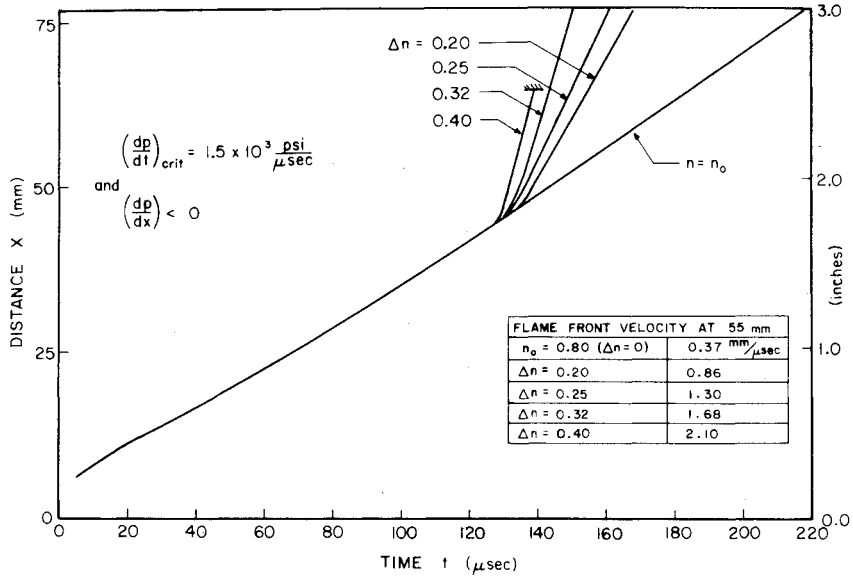


**Fig. 8 Flame front locus resulting from an abrupt change (at the critical pressure gradient) in the burning rate exponent (limited to the localized region of the presure front, using a compressible solid).**

at some imposed critical condition, in this case where the gas pressure exceeds 0.35 GPa (50 kpsi). The shape of the flame front is now beginning to resemble the data of Bernecker and Price[4] although the ignition front velocity is still less than those reported in Ref. 6. (This case did not proceed to completion due to the same type of numerical instabilities described in Ref. 6.)

In order to limit the effect of the nonlinear source-term increase, which causes the numerical integration breakdown, case c was repeated by assuming only a 5% increase in the exponent $n$. As expected, the integration proceeded normally. As the pressure history profiles shown in Fig. 7 indicate, there is a significant increase in the level of the gas pressure shortly after the propellant burning rate is increased. An effect of this pressure wave increase on the motion of the flame front is a predicted break in the slope of the flame front that occurs for 10 $\mu$s after the critical pressure has been predicted. However, when the location of the pressure front is defined as the point of maximum rate of change of slope on the pressure time plot as was done by Bernecker and Price,[4] it can be seen that the pressure wave moves ahead of the flame at about the time of the change in the burning rate exponent. Despite the lack of high flame velocities after this type of transition (which may be due to the relatively low initial solids loading treated here), this flame front/pressure front exhibits a remarkable similarity to the experimental results of Bernecker and Price.[4]

Changes in burning rate proportionality constant $b$ do not show as dramatic a change in the slope of the flame front simply because the assumed increased values of $b$ were not as large as the increase due to the pressure-power law function. Additionally an assumed abrupt change in the solid density at some prescribed high pressure produces results similar to those found when the addition of a state equation was made, namely, a reduction in the slope of the flame front instead of an increase.

The previous section introduced a possible mechanism which yields results supportive of the first DDT scenario described in Ref. 6. But in all cases described to this point there was no evidence of a compression wave moving through the unignited portion of the bed. This meant that conditions for the second DDT scenario were not being modeled. Modification necessary to obtain this type of physical effect included the introduction of a new compaction resistance law, a modification of the solid phase momentum equation, and the assumption that a solid phase stress wave will move through the unignited part of the bed at the solid phase sound speed behind the wave. The details of each of these new assumptions are presented in Ref. 6.

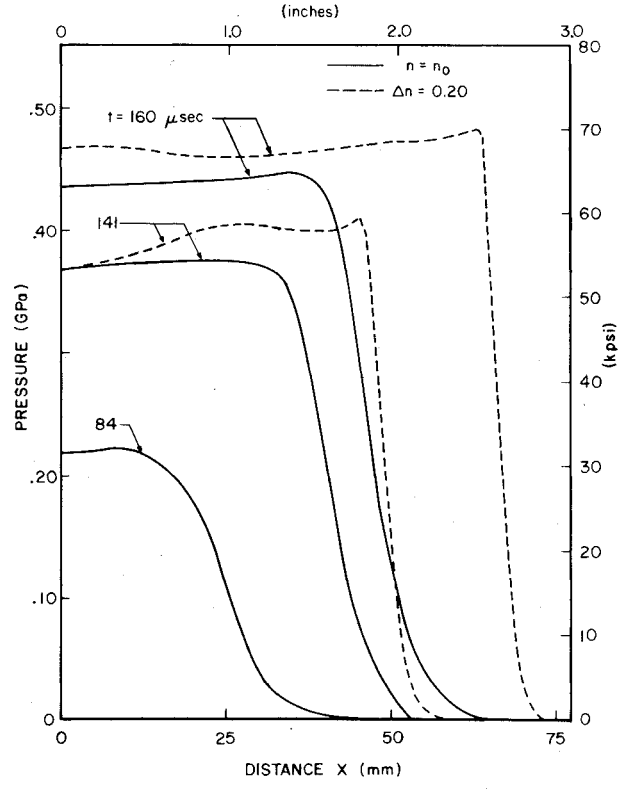


**Fig. 9 Pressure distribution history as a function of burning rate exponent change (limited to the localized region of the pressure front).**

## IV. Conclusions

### Summary of Investigations

The work presented in this report represents a continuation of the efforts begun by Krier-Gokhale[1] and Krier-Kezerle[2] to correctly model the deflagration-to-detonation transition phenomenon. In these previous studies, the investigation was focused on determining a set of governing equations which properly described the peculiar nature of the flow and with properly incorporating these equations into a numerical integration scheme. This study essentially began with these developed codes and attempted to determine the sensitivity of the various assumptions made previously in order to better understand the properties of the flow which are necessary to correctly model a smooth transition to detonation.

The work presented has, among other things, served the purpose of focusing attention on various aspects of the DDT phenomenon which will require a much more thorough understanding before any significant confidence in the results can be obtained.

For example, it is unknown at this time if the fundamental relationships for the drag and heat transfer are valid at the high Reynolds numbers encountered in this type of flow. Results presented previously show what kind of effect a reduction in the drag relation can have on the progress of the flow. It is also uncertain what effect the large gas pressures have on the burning rate of these types of propellants. That is, dynamic burning rate phenomena may negate the use of the rate equation used in Ref. 6.

The large pressure buildups in the short time periods which occur in this type of problem would be expected to create some sort of dynamic compaction in the porous bed. But again, the nature of this compaction is not fully understood and therefore cannot be modeled properly in this code. Further experimentation will need to be conducted if questions of this type are to be answered (Ref. 9).

Further improvements in the code itself can be obtained with the introduction of concepts commonly used in detonation physics. This would include the use of a revised gas generation term which reflects the increased mass transformation rates which occur in a detonation.[11] Use would also need to be made of detonation chemistry which allows for the shock initiation of the types of materials being considered here. An example of the possible use of this concept is to allow an abrupt change in the burning rate exponent as was done in Sec. III. However, this increased burning rate probably should be limited to what could be called the shock front, that is, the exponent increase should be confined to that region where the gas pressure is increasing at some critical rate with respect to time. As has been shown throughout Sec. II, this type of zone is always found to be closely coupled to the ignition front.

An indication of the results of this type of localized burning rate increase are presented in Figs. 8 and 9. Specifically, the exponent $n$ is increased from $n_0$ to $n_0+n$, only when $dP/dt>0.01$ GPa/$\mu$s ($1.5\times10^3$ psi/$\mu$s) and only if the pressure gradient, $dP/dx$ is negative. Although these results resemble those shown in Sec. III, the logic used here models a sequence of events which is much closer to the circumstances known to occur in a detonation. The flame front velocities which occur after the break in its slope were found to be constant, which is another important characteristic of a detonation. And finally, the crossing of the flame front by the pressure front before the break in the flame front slope was found to occur in all cases presented in Fig. 8. But owing to the means by which the reaction zone was defined (in this case, the restriction that $dP/dx<0$), the pressure front eventually dropped below the flame front for the higher values of $\Delta n$ as the burn progressed. This was caused by the fact that increases in $\Delta n$ resulted in a steepening of the pressure-distance curve, which in turn caused the reaction zone to become narrower in extent and thus less powerful in its motion through the bed. This problem can be rectified by using a somewhat more complicated means of defining the reaction zone which will allow the thickness of the zone to be maintained at a desired level independent of the pressure-distance curve.

It should be noted that in all cases presented in this paper the initial solid loading is only 60% (porosity $\phi=0.40$) while the experiments of Bernecker and Price[4] had initial solids loading of approximately 80-90%. To treat values of loading higher than 74% one must assume that a bed of multisized particles is being used. This leads to a number of difficulties concerning the proper method of partitioning flow properties such as the interphase drag and heat transfer. (For a discussion of their potential solution, see Ref. 10.)

Another aspect which should be looked into both as a means of improving this code in particular and for solving this DDT problem in general is to review again the numerical scheme itself. The full effects of the numerical smoothing function have not been exhaustively studied and refinements are certainly not out of the question. The use of a "rezoning" technique in which either the grid spacing or the time step or both are decreased in regions of severe gradients may prove to be very valuable in obtaining better accuracy for the same or even lower computing time and costs. Reasonable solutions may not be acquired from any of these suggestions until larger computers become available since many of the calculations encountered thus far entailed calculating small differences of large numbers.

Finally, it should again be pointed out that although a number of difficulties and constraints have been discussed in this section, many of the problems would not be recognized as such without the progress that has been made in this work. Further research into these problems will certainly make progress towards a solution to the overall production of deflagration-to-detonation transition.

## Appendix: Constitutive Relations

This section describes in more complete detail the constitutive relations and criteria outlined in Sec. II. Due to the selection of separate energy equations for each phase of the flow it becomes impractical to use the method of Kuo et al.[12] to define an ignition temperature based on the solution of the heat conduction equation for the particles. Instead, the method proposed by Krier et al.[13] in which a "bulk particle temperature," defined as the average temperature of the solids, was used as the critical variable for determining ignition. Under this approach, ignition occurs once the bulk temperature reaches some critical $T_{ign}$ which is less than the critical surface temperature used by Kuo et al.[12]

Convective heat transfer between the hot gases and the particles made use of Denton's[14] heat transfer coefficient

$$h_{pg}=0.65\left(\frac{K_g}{2r_p}\right)\left(\frac{\rho_g\,|\,U_g-U_p\,|\,(\phi)\,(2r_p)}{\mu_g}\right)^{0.7}(Pr)^{0.33} \quad \text{(A1)}$$

where $K_g$ is the thermal conductivity of the gas, $\mu_g$ is the viscosity of the gas, and $Pr$ is the Prandtl number of the gas phase.

Owing to questions concerning the alteration of the boundary layer around a burning particle which in turn alters the convective heat transfer, it has been assumed that the above value for the heat transfer coefficient is reduced, once the particle is ignited, to one-tenth of the value used if the particle were not burning.

The drag coefficient, $f_{pg}$, used in this investigation is that devised by Kuo and Nydegger,[15] namely,

$$\bar{F}=\frac{\mu_g(U_g-U_p)}{(2r_p)^2}\left(\frac{1-\phi}{\phi}\right)^2\underbrace{\left[276.23+5.05\left(\frac{Re_p}{1-\phi}\right)^{0.87}\right]}_{f_{pg}} \quad \text{(A2)}$$

where $Re_p$ is the Reynold's number based on the particle radius

$$Re_p=2r_p\rho_g\phi\,|\,U_g-U_p\,|\,/\mu_g \quad \text{(A3)}$$

The value for the gas viscosity, $\mu_g$, used in the last three equations was assumed to vary with temperature only. Ideally, the variation should be with respect to both temperature and pressure due to the extremely high values for both of these parameters. However, no such relation could be found so the following relation was settled on as being the most applicable.

$$\mu_g = \mu_{g_0} (T_g / T_{g_0})^{0.65} \quad \text{(A4)}$$

where $\mu_{g_0}$ and $T_{g_0}$ are initial conditions for each variable.

The burning rate law used throughout this work is the simple pressure dependent relation

$$\dot{r} = b_1 (P_g)^n \quad \text{(A5)}$$

where $b_1$, $b_2$ and $n$ are constants. Occasional use was made of a variation of this law

$$\dot{r} = b_3 (T_g / T_{g_0})^m (P_g)^n \quad \text{(A6)}$$

which will be noted when used.

## Acknowledgment

This work was supported by the Air Force Office of Scientific Research under Contract No. AFOSR 77-3336; Dr. Leonard H. Caveny, Project Director.

## References

[1] Krier, H. and Gokhale, S. S., "Modeling of Convective Mode Combustion to Predict Detonation Transition," *AIAA Journal,* Vol. 16, Feb. 1978, pp. 177-183.

[2] Krier, H. and Kezerle, J., "A Study of Unsteady One-Dimensional Two-Phase Reactive Particle Flow," Department of Aeronautical and Astronautical Engineering, University of Illinois, Urbana, Ill., Report UILU-Eng 77-0517 (1977); also, *Proceedings of the 17th Symposium on Combustion,* The Combustion Institute, Pittsburgh, Pa., 1979, pp. 23-34.

[3] Krier, H., Gokhale, S., and Hoffman, S., "Unsteady Two-Phase Flow Analysis Applied to Deflagration-to-Detonation Transition," AIAA Paper 78-1013, July 1978.

[4] Bernecker, R. R. and Price, D., "Studies in the Transition to Detonation in Granular Explosives," *Combustion and Flame,* Vol. 22, 1974, Parts I-II, pp. 111-129, Part II, pp. 161-170.

[5] Bernecker, R. R., Price, D., and Sandusky, H. W., "Burning to Detonation Transition in Porous Beds of a High-Energy Propellant," *Proceedings of the 16th JANNAF Combustion Meeting,* Chemical Propulsion Information Agency, Vol. I, 1979, pp. 51-78.

[6] Hoffman, S. J. and Krier, H., "Fluid Mechanical Processes of DDT in Beds of Porous Reactive Solids," University of Illinois, Tech. Rept. AAE 80-2 (UILU-Eng 80 0502), April 1980.

[7] Wallis, G. B., *One-Dimensional Two-Phase Flow,* McGraw-Hill Book Co., New York, 1969.

[8] Kuo, K. K. and Summerfield, H., "High Speed Combustion of Mobile Granular Solid Propellants," *15th Symposium on Combustion,* The Combustion Institute, Pittsburgh, Pa., 1974, pp. 515-525.

[9] Kuo, K. K., Yang, V., and Moore, B. B., "Intergranular Stress, Particle-Wall Friction and Speed of Sound in Granular Propellant Beds," *Journal of Ballistics,* Vol. 4, No. 1, 1980, pp. 697-730.

[10] Gokhale, S. S., *Theoretical Studies in the Transition to Detonation of Granular Solid Propellants,* Ph.D. Dissertation, University of Illinois at Urbana-Champaign, Ill., Department of Aeronautical and Astronautical Engineering, May 1980.

[11] Fickett, W. and Davis, W. C., *Detonation,* University of California Press, Berkeley, Calif. (Los Alamos Series in Basic and Applied Sciences), 1979.

[12] Kuo, K. K., Vichnevetsky, R., and Summerfield, M., "Theory of Flame Front Propagation in Porous Propellant Charges," *AIAA Journal,* Vol. 2, April 1973, pp. 444-451.

[13] Krier, H., Rajan, S., and Van Tassell, W. F., "Flame Spreading and Combustion in Packed Beds of Propellant Grains," *AIAA Journal,* Vol. 14, March 1976, pp. 301-309.

[14] Denton, W. H., "The Heat Transfer and Flow Resistance for Fluid Flow Through Randomly Packed Spheres," *ASME Transactions,* 1951, p. 370.

[15] Kuo, K. K., and Nydegger, C. C., "Flow Resistance Measurements and Correlation in a Packed Bed of Ball Propellants," *Journal of Ballistics,* Vol. 2, No. 1, 1978, pp. 1-26.